Catalytic evidence of the core/shell structure of bimetallic Pd/Rh colloids

Christian Bergounhou,[a] Claudine Blandy,[a] Robert Choukroun,*[a] Pierre Lecante,[b] Christian Lorber[a] and Jean-Louis Pellegatta[a]

Received (in Montpellier, France) 13th October 2006, Accepted 23rd November 2006
First published as an Advance Article on the web 19th December 2006
DOI: 10.1039/b614910c

The co-reduction of $[Rh(C_2H_4)_2Cl]_2$ and $[Pd(\eta^3\text{-}C_3H_5)Cl]_2$ with vanadocene $[Cp_2V]$ in THF, and in presence of poly(vinylpyrrolidone) (PVP), gives bimetallic PVP-protected Rh/Pd colloids. HREM and WAXS experiments show a narrow size distribution centered near 2 nm, indicating the existence of bimetallic particles rather than physical mixtures of monometallic ones. CO chemisorption, followed by IR in CH_2Cl_2, as well as catalytic hydrogenation of quinoline and phenylacetylene, followed by GC in CH_2Cl_2 or CH_2Cl_2/H_2O, confirm the presence of core/shell-structured bimetallic colloids, with Pd atoms surrounded by Rh atoms.

Introduction

Many efficient systems are known to generate nanoparticles.[1] This chemistry (and the physical properties) has been summarized in a number of excellent reviews and various informative contributions to textbooks. The applicability and success of these systems often depends on their preparative accessibility.

Bimetallic nanoparticles have been investigated with great interest due to their interesting physical and chemical properties resulting from the combination of two kinds of metals. To the best of our knowledge, the structure of colloidal dispersions of Rh/Pd bimetallic clusters were previously prepared by refluxing a solution of their salts in water/ethanol in the presence of poly(vinylpyrrolidone) (PVP) and studied by the extended X-ray absorption fine structure (EXAFS) technique.[2] The formation of Rh and Pd clusters, as well as bimetallic Rh/Pd colloids, was demonstrated. The Rh atoms of the bimetallic systems were highly dispersed on the surface.

Since Rh and Pd are well known for their high activity in numerous processes,[3] we decided to use the chemical knowledge gained from our early work on Rh and Pd colloids and employ it to the synthesis of bimetallic Rh/Pd nanoparticles. Indeed, we reported previously an organometallic route to access Rh and Pd nanoparticles embedded in PVP *via* the reaction of $[Rh(C_2H_4)_2Cl]_2$ or $[Pd((\eta^3\text{-}C_3H_5)Cl]_2$ with vanadocene (as a reducing agent) in THF in the presence of PVP.[4] These previous investigations account for our interest in the preparation Rh/Pd bimetallic colloids *via* our preparative synthesis. Rh/Pd bimetallic nanoparticles have been synthesized using different ratios of organometallic Rh and Pd precursors, and the series has been studied so as to attempt to elucidate the model core/shell of these particles.

[a] *Laboratoire de Chimie de Coordination du CNRS (UPR 8241), lié par convention à l'Université Paul Sabatier, 205 route de Narbonne, 31077 Toulouse Cedex 4, France. E-mail: choukrou@lcc-toulouse.fr; Fax: +33 561 55 30 03; Tel: +33 561 33 31 61*
[b] *CEMES-LOE-CNRS, 29 rue Jeanne Marvig, BP 4347, 31055 Toulouse Cedex, France*

Results and discussion

Physical characterization of the colloids

In recent work,[4] Rh and Pd colloids were prepared according to the reaction in Scheme 1, in the presence of PVP (K30-PVP) as protecting polymer, and isolated as black solids. Both colloids were characterized by HREM and wide angle X-ray scattering (WAXS), which evidenced the fcc structure inside well-dispersed particles.

The Rh/Pd bimetallic colloids here described were obtained *via* a similar process. The co-reduction of $[Rh(C_2H_4)_2Cl]_2$ and $[Pd(\eta^3\text{-}C_3H_5)Cl]_2$ has been performed in THF with a stoichiometric amount of $[Cp_2V]$ as reducing agent, and in the presence of K30-PVP polymer used to trap the colloids (Scheme 2). Different ratios of the organometallic precursors were tested and, according to elemental analysis, a wide range of compositions in the sample Rh/Pd alloys were obtained. The Rh/Pd preparation, series **A** for catalytic purposes, used in this work (*vide infra*) contained, for example, particles as Rh-rich as $RhPd_{0.2}$ and as Pd-rich as $RhPd_{12.5}$.

$$[Cp_2V] + 1/2\ [Rh(C_2H_4)_2Cl]_2 \xrightarrow[PVP]{THF} \text{"[Rh/PVP]"} + [Cp_2VCl] + 2\,(C_2H_4)$$

$$[Cp_2V] + 1/2\ [Pd(\eta^3\text{-}C_3H_5)_2Cl]_2 \xrightarrow[PVP]{THF} \text{"[Pd/PVP]"} + [Cp_2VCl] + (C_3H_6)$$

Scheme 1 Synthesis of the monometallic nanoparticles.

$$(x+y)\,[Cp_2V] + x\,[Rh(C_2H_4)_2Cl]_2 + y\,[Pd(\eta^3\text{-}C_3H_5)_2Cl]_2 \xrightarrow[PVP]{THF} \text{"}[Rh_xPd_y/PVP]\text{"} + (x+y)\,[Cp_2VCl] + x\,(C_2H_4) + y\,(C_3H_6)$$

	A1	A2	A3	A4	A5	A6	A7
Composition	Pd	$RhPd_{12.5}$	$RhPd_{4.5}$	$RhPd_{1.4}$	$RhPd_{0.5}$	$RhPd_{0.2}$	Rh

Scheme 2 Synthesis of the bimetallic nanoparticles.

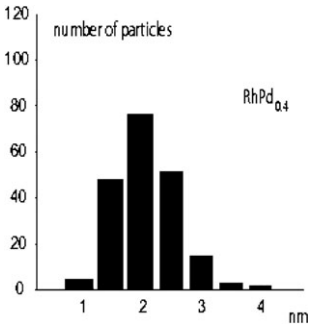

Fig. 1 Histogram showing the size distribution of a $RhPd_{0.4}$ sample.

This series **A** was completed by other Rh/Pd bimetallic colloids (see below for TEM and HREM images) and by physical mixtures of Rh and Pd colloids, independently prepared according to our previous procedures:[4] **M1**: $RhPd_{4.3}$, **M2**: $RhPd_{1.8}$ and **M3**: $RhPd_{0.7}$. Mixtures **M** of these different compositions have been prepared to probe their physical and chemical properties compared to alloy series **A**.

TEM and HREM images obtained for several **A** compositions showed well-dispersed microcrystalline particles. From measurements of over 200 particles for different RhPd compositions ($RhPd_{11}$, $RhPd_{4.5}$, $RhPd_{0.4}$ and $RhPd_{0.7}$), the average size from electron microscope observations was approximately 1.9 nm, with a relatively narrow size distribution (Fig. 1). Their mean diameter was nearly the same, irrespective of the composition of the bimetallic colloids. However, if fringes were precisely observed for particles of different composition (Fig. 2), their lack of regular periodicity did not allow the structure of the particles to be determined, despite the large number of particles investigated. The electron diffraction pattern obtained for particles $RhPd_{1.5}$ is shown in Fig. 2 (insert), and also illustrates the lack of periodicity inside the particles.[5] Their average composition, by the analysis of a group of particles by EDX attached to a HREM, corresponds well to the composition obtained by analytical analysis (though we were unable to probe the composition of individual particles). This analytical method is not sensitive enough to elucidate the detailed chemical order in such small bimetallic nanoparticles, and other physical and chemical analysis methods must be combined.

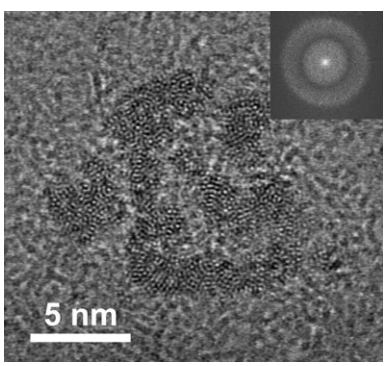

Fig. 2 HREM micrograph of $RhPd_{1.5}$, revealing the fringes in the particles and the microdiffraction pattern observed (insert).

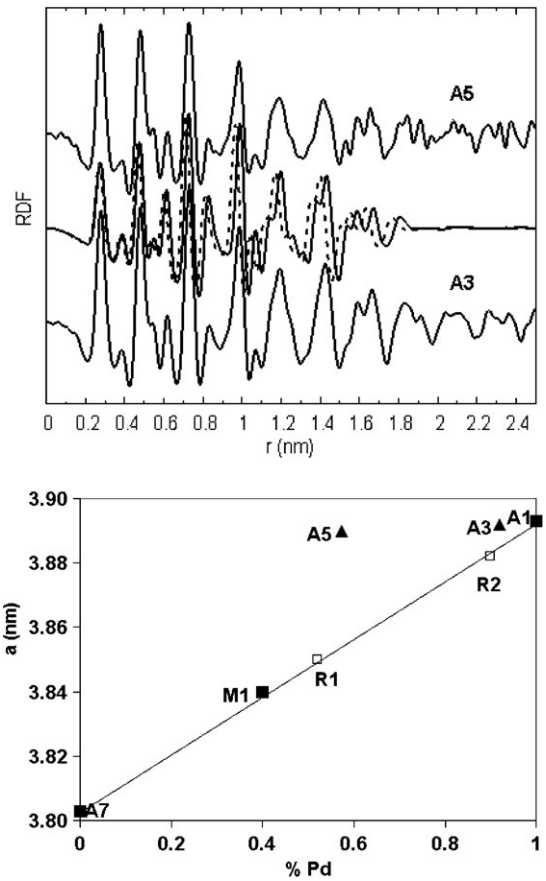

Fig. 3 Upper: Top and bottom experimental RDFs for **A5** and **A3**, respectively; middle, computed RDF from bulk Pd (solid line) and Rh (dotted line). Lower: *a* parameter *vs.* composition; reference alloys (symbol ϒ) follow Vegard's law (linear change with Pd/Rh ratio).

Structural characterization of samples **A3** and **A5**, mixture **M1**, and **A1** with **A7** as a standard, was undertaken by WAXS in the solid-state.[6] Such small particles only generate broad patterns, which do not allow for accurate determination of lattice parameters in the reciprocal space. However, after data reduction and Fourier transformation, performed similarly to previous studies,[7] well-detailed experimental radial distribution functions (RDFs) were obtained for **A3** and **A5**, which gave clear evidence of an fcc organization, also present in both bulk Rh and Pd (Fig. 3, upper). From the coherence length, the average diameter is estimated to be 2 nm, in agreement with TEM.

We then matched simulated RDFs, computed from fcc models, with the experimental ones in order to determine the lattice parameter *a* in the nanoparticles for the different compositions. The results are reported in Fig. 3 (lower), together with values reported for the pure metals and the different alloys at room temperature. The accuracy of our values is estimated to be 0.001 nm. Two very different behaviours can be observed. For the physical mixture **M1**, *a* closely follows Vegard's law, drawn from reference structures (**R1** and **R2**, provided by the ICSD database, and **A1** and **A7**), while for **A3** and **A5**, values are significantly larger. In fact, for both samples, *a* remains very close to the value for pure Pd, which is

a very strong indication of segregation of the elements in the particles. In such a view, these should include a Pd (or Pd-rich) core, imposing the lattice parameter, surrounded by a stretched Rh (or Rh-rich) shell. Of course, a more complex organization, following a different sequence of alloyed layers, cannot be excluded nor evidenced by WAXS alone, provided they include a Pd core.

To go further into the characterization of these bimetallic colloids and to probe their bimetallic synergistic effect, we have taken advantage of the chemical reactivity of bimetallic systems already observed in nanoparticles. Characterization of the surface composition can be realized by chemical probes, such as carbon monoxide, and catalytic hydrogenation.

CO chemisorption

IR studies have already been used as a technique to determine the surface composition of bimetallic nanoparticles.[1f,8] FTIR spectra of CO adsorbed at a fixed concentration of Rh and Pd monometallic colloids dissolved in a solvent were collected, as well as spectra of the bimetallic colloids and of physical mixtures at a nearly identical concentration. Comparison of the intensities of the bands is facilitated by using CH_2Cl_2 solutions containing the same total content of metallic atoms. The attributing of the CO frequencies in the Rh and Pd colloids is based on previous work on surfactant-stabilized Rh colloids, PVP-Rh colloids and Pd nanoparticles formed in block copolymer micelles.[1f,9] IR spectroscopy of adsorbed CO on stabilized Rh colloids in CH_2Cl_2 solvent lead to a spectrum (Fig. 4, line a) that exhibited six different bands, corresponding to free CO in solution (used as a standard at 2135 cm^{-1}) and three different Rh–CO moiety species: geminal/terminal (2070 (m), 2045 (m), 1990 (m) and 1975 (m) cm^{-1}) and bridged (1850 cm^{-1} (broad, m)). Some shoulders appeared at 2083, 2040 and 2050 cm^{-1}, which could not be attributed with certainty to the clusters $Rh_4(CO)_{12}$ (4 weak bands at 2074, 2069, 2044 and 1886 cm^{-1}) or $Rh_6(CO)_{16}$ (1811 cm^{-1}).[10] A CO chemisorption study of PVP-Pd colloids in CH_2Cl_2 solution (Fig. 4, curve e) showed free CO in solution (2135 cm^{-1}) and two species of CO coordinated to the surface: terminal/geminal (2065 and 2050 cm^{-1}) and bridged (1930 cm^{-1}).[9] IR spectra of CO adsorbed on bimetallic PVP-Rh/Pd colloids in CH_2Cl_2 were also collected for different Rh concentrations (Fig. 4, curves b–d). Only one broad band was observed in the range 1850–1950 cm^{-1}, and its maximum shifted about 1925–1865 cm^{-1} when the ratio of Pd decreased. These data suggest that Pd

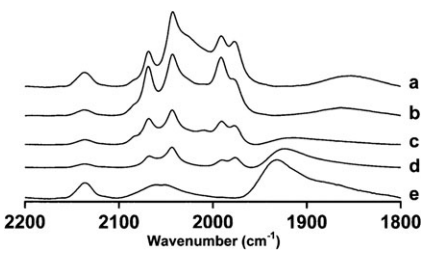

Fig. 4 IR spectra of CO adsorbed on: (a) Rh-PVP and (e) Pd-PVP, and on bimetallic Rh/Pd-PVP colloids containing (b) 84% Rh, (c) 44% Rh and (d) 12% Rh, respectively.

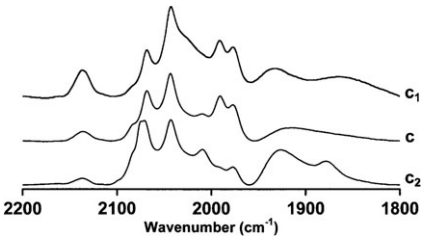

Fig. 5 IR spectra of CO adsorbed on Rh/Pd-PVP colloid (c), a mixture of monometallic colloids (c_2) and theoretical mixture (c_1) with 44% Rh and 56% Pd in each case.

nanoparticles are masked progressively by Rh nanoparticles, which prevent the observation of Pd–CO bands.

The comparison in Fig. 5 of the CO bridged region spectra of bimetallic Rh/Pd colloids with nearly the same composition (44% Rh/56% Pd) indicates two bands (1890 and 1915 cm^{-1}) for the mixture of both monometallic colloids (curve c_2) and only one large band (1925 cm^{-1}) for the corresponding alloy (curve c). On the theoretical spectrum (c_1), obtained by the combination of the Rh and Pd spectra (44% Rh, 56% Pd), we observe two bands, as in the c_2 spectrum. Therefore, we can confirm that spectrum c corresponds to the existence of bimetallic particles rather than physical mixtures of monometallic ones, the surface of the nanoparticles being essentially covered by Rh atoms.

Catalytic hydrogenation of quinoline and phenylacetylene substrates

Characterization of the surface composition of the nanoparticles could be helped by a catalytic process.[11] Our aim was to compare the catalytic properties of the bimetallic colloids **A** and mixtures **M** to provide chemical evidence that **A** and **M** are of different nature, and that a clear synergistic effect of Rh and Pd is observed in the bimetallic colloids **A**.

The first challenge was to find an ideal substrate, the hydrogenation of which would be activated by one metal and inhibited by the second. In this respect, quinoline and phenylacetylene are, respectively, easily hydrogenated in presence of Rh and Pd colloids as catalysts.

Indeed, our preliminary kinetic measurements of the hydrogenation of quinoline with Rh-PVP catalyst showed that quinoline was easily hydrogenated into 1,2,3,4-tetrahydroquinoline (rate r = 180 mol h^{-1} $atom^{-1}$) but not with Pd-PVP catalyst (r = 22 mol h^{-1} $atom^{-1}$). In contrast, kinetic measurements of phenylacetylene hydrogenation into styrene with Rh-PVP is less active (r = 315 mol h^{-1} $atom^{-1}$) than with Pd-PVP catalyst (r = 1321 mol h^{-1} $atom^{-1}$). Therefore, quinoline and phenylacetylene are ideal candidates for investigating the core/shell structure of the bimetallic colloid nanoparticles.

In previous work, the hydrogenation of phenylacetylene to styrene and styrene to ethyl benzene by Rh nanoparticles led to similar rates and with linear variations of concentration with time, indicating a zero-order with respect to the substrates.[12]

The same linear variation was obtained for the hydrogenation of phenylacetylene and quinoline using Rh or Pd

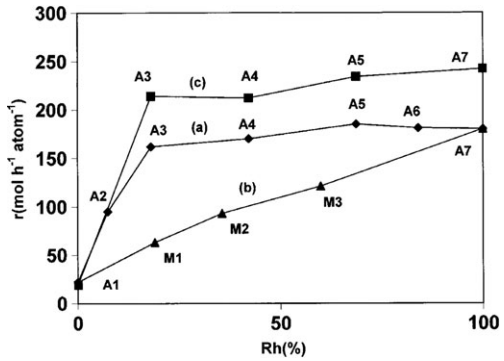

Fig. 6 Hydrogenation of quinoline under biphasic conditions (CH_2Cl_2/H_2O) for bimetallic colloids (line a), under biphasic conditions (CH_2Cl_2/H_2O) for mixtures of monometallic colloids (line b) and under monophasic conditions (CH_3OH) for bimetallic colloids (line c).

nanoparticles, therefore corresponding to a zero-order with respect to both substrates. The catalytic hydrogenation reactions were also examined for catalyst concentration and hydrogen pressure effects. By increasing the dihydrogen pressure (2, 3 and 4 bar at 40 °C), the rate of quinoline hydrogenation was enhanced (r = 915, 1290 and 2040 mol h^{-1} $atom^{-1}$), with a first-order dependence. The same effect had already been observed with phenylacetylene (r = 2.5 and 1.3 mol h^{-1} $atom^{-1}$ for 7 and 3.5 bar, respectively, at 60 °C).[12] The effect of catalyst concentration also indicates a first-order dependence for both systems. So, by using the same kinetic model for mono and bimetallic systems, the rate law for all catalysis can be written as: $r = k \times [\text{catalyst}] \times P_{H_2}$ where k = apparent rate constant and P = partial pressure.

The hydrogenation of quinoline was tested using monophasic liquid systems (CH_3OH or CH_2Cl_2) and a biphasic liquid system (CH_2Cl_2/H_2O), where the catalyst was dispersed in the aqueous phase. The reaction was monitored by GC. In Fig. 6, we can compare the hydrogenation rates obtained when biphasic conditions (CH_2Cl_2/H_2O) were used for different Rh/Pd-PVP concentrations, calculated in terms of % Rh atom fraction (line a: **A1**–**A7**), with the values corresponding to the same catalysts dispersed in methanol (line c).

It is interesting to note that the reactivity is slightly improved in presence of methanol due to a better dispersion of the colloid and/or higher solubility of dihydrogen in methanol. The different concentrations corresponding to each entry are reported in Table 1.

Fig. 6, line b corresponds to simple physical mixtures of monometallic Pd and Rh catalysts (**M1**, **M2** and **M3**) of different composition using a two-phase system (CH_2Cl_2/H_2O) (see Table 1).

The observed rate is the sum of the two rates obtained for the catalysis of individual Rh/PVP and Pd/PVP systems, and is, for this reason, directly dependent on the relative composition of the mixture of the two colloids. So, the expected and observed variation is linear (line b).

It appears that, for a given composition, the bimetallic catalysts are more active than a simple mixture of monometallic colloids (line a > line b). At this point, enhancement of catalytic activity could suggest the selective locations of Rh atoms in the bimetallic Pd/Rh nanoparticles.

It can be seen in Table 1 that the addition of Rh enhanced the activity of biphasic conditions (**A1**–**A3**), as well as of monophasic ones (CH_3OH or CH_2Cl_2), and that for a Rh content of greater than about 20%, the activity remained similar to that of pure Rh colloids **A7**.

Exposure of colloid **A4** to air over 3 d did not change the hydrogenation rate in the CH_2Cl_2/H_2O system; this gives evidence of the absence of significant oxidation of the particles.

The hydrogenation of phenylacetylene was tested using monophasic systems (CH_3OH or CH_2Cl_2).[13] The catalysis was stopped at the first step of the reaction, corresponding to the formation of styrene, on account of the same hydrogenation rate value of styrene into ethylbenzene.

Fig. 7 reports the hydrogenation rates of phenylacetylene obtained from Rh/Pd-PVP samples of different composition in CH_3OH (line a, samples **A1**, **A4**, **A8** and **A7**) and CH_2Cl_2 (line b, samples **A1**, **A3**, **A4** and **A7**). It is interesting to note that the rate values correspond to an opposite situation compared to that obtained for quinoline hydrogenation; monometallic Pd colloids are more effective for phenylacetylene hydrogenation, but when Rh content is added, the catalytic activity decreases to reach the activity of pure Rh nanoparticles when only 20% Rh is present in the bimetallic colloid. Line b′ of Fig. 7 is directly dependent upon the relative composition of the mixture of the two colloids, and corresponds to the sum of the two catalytic rates due to Rh-PVP and Pd-PVP; the rate value expected for a simple physical mixture of monometallic Pd and Rh catalysts (**M3**) is indeed observed, showing again the

Table 1 Hydrogenation rate values of quinoline for monometallic and bimetallic colloids (**A1**–**A7**), and for physical mixtures of monometallic colloids (**M1**–**M3**) in different solvents

					Rate/mol h^{-1} $atom^{-1}$		
Catalyst	Rh (%wt)	Pd (%wt)	Atom fraction Rh (%)	Relative proportions	CH_2Cl_2/H_2O	CH_3OH	CH_2Cl_2
A1	0.00	8.43	0.0	Pd	22	19	24
A2	0.80	10.30	7.4	$RhPd_{12.5}$	95		
A3	2.45	11.45	18.1	$RhPd_{4.5}$	162	214	125
A4	5.56	7.87	42.2	$RhPd_{1.4}$	170	212	158
A5	6.96	3.28	68.7	$RhPd_{0.5}$	185	234	
A6	6.30	1.20	84.0	$RhPd_{0.2}$	181		
A7	5.00	0.00	100.0	Rh	180	242	147
M1			19.0	$RhPd_{4.3}$	63		
M2			35.6	$RhPd_{1.8}$	93		
M3			60.0	$RhPd_{0.7}$	121		

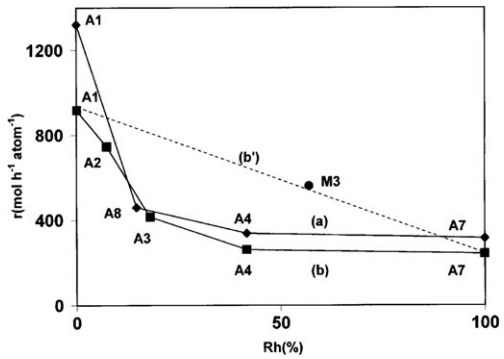

Fig. 7 Hydrogenation of phenylacetylene for bimetallic colloids in CH_3OH (line a), CH_2Cl_2 (line b) and for the **M3** mixture of monometallic colloids in CH_2Cl_2 (line b′).

different catalytic behaviours of bimetallic Rh/Pd nanoparticles and their physical mixtures.

Catalyst **A4** was recovered by evaporation after catalysis. Observation by TEM showed well-dispersed nanoparticles with a narrow size distribution centred near 2–2.5 nm, which is quite similar to that obtained before catalysis.

Conclusions

The catalytic results obtained in the hydrogenation of quinoline showed, unambiguously, a significant enhancement of the activity by the bimetallic colloids **A**, in comparison to the linear additive effect of Rh and Pd observed for the physical mixtures **M**. For the hydrogenation of phenylacetylene, Rh atoms could be considered as inhibitors of the bimetallic catalyst. The maximum or minimum activity of the bimetallic colloids were exhibited at nearly $RhPd_4$, depending on the substrate. For the highest Rh content, the activity of the bimetallic colloids could be considered monotonic and similar to that of the pure Rh colloids. This suggests that Rh atoms are preferentially at the surface on the bimetallic colloids, as a shell that serves as a catalytic promoter for the quinoline, or, *a contrario*, a protective shell over the Pd core that prevents the catalytic hydrogenation of the phenyl acetylene (bearing in mind that quinoline and phenyl acetylene are almost specifically hydrogenated in the presence of Rh or Pd nanoparticles).[14] A similar result was observed in the catalytic hydrogenation of crotonic acid by a bimetallic PtRh system, in which a $PtRh_4$ colloid showed the maximum activity.[15]

In summary, we have found that the organometallic one-pot route, which uses variable mixtures of Rh and Pd precursors $[M(\text{I})Cl]_2$ (M = $Rh(C_2H_4)_2$, $Pd(C_3H_5)$, and Cp_2V as a reducing agent in the presence of PVP, gave core/shell Pd/Rh bimetallic colloids of different composition and similar size (nearly 2 nm). HREM showed the crystallinity of these bimetallic colloids from their fringes, whereas WAXS techniques demonstrated the core/shell Pd/Rh structure of these nanoparticles. By combining chemical techniques—CO adsorption and catalytic hydrogenation—the synergistic effect of both metals was emphasized, possibly due to the selective locations of the Rh atoms in the core/shell structure of these bimetallic nanoparticles.[14]

Experimental section

Synthesis and characterization of the nanoparticles

Synthesis of the nanoparticles was carried out under an inert Ar-atmosphere in a glove box. The Rh and Pd nanoparticles embedded in PVP were prepared according to our previous published procedure.[4] The different mixtures **M** were prepared from weighted **A1** and **A7** colloids dissolved in MeOH. After stirring 1–2 h, the solvent was evaporated and the dark grey solid dried *in vacuo*. The bimetallic colloids were prepared by the simultaneous reduction of $[Rh(C_2H_4)_2Cl]_2$ and $Pd(\eta^3\text{-allyl})Cl]_2$ with $[Cp_2V]$ in presence of poly(*N*-vinyl 2-pyrrolidone) (PVP, K-30) typically as follows. A mother solution of 800 mg PVP in THF (20 mL) was divided into two equal volumes and added to a THF solution (10 mL) of 174 mg $[VCp_2]$ (0.96 mmol), and to a THF solution (10 mL) containing 95 mg of freshly prepared $[Rh(C_2H_4)_2Cl]_2$ (0.24 mmol) and 86 mg of $[Pd(\eta^3\text{-allyl})Cl]_2$ (0.24 mmol). Under vigorous stirring, the Cp_2V solution was added dropwise to the other solution. The resulting combined solution turned black and stirring was continued for 12 h, during which time the colloids precipitated. The solution was concentrated to 5 mL, and toluene (15 mL) was added. The resulting black solid, PVP-protected Rh/Pd colloids, was filtered and washed thoroughly (10 mL toluene/THF 3 : 1, 3 × 10 mL toluene/THF 2 : 1 and 10 mL toluene/THF 1 : 1). The black solid thus obtained was finally dried (710 mg). Elemental analysis: **A1**: Pd 8.43%; **A2**, $RhPd_{12.5}$: Rh 0.8%, Pd 10.30%; **A3**, $RhPd_{4.5}$: Rh 2.45%, Pd 11.45%; **A4**, $RhPd_{1.4}$: Rh 5.56%, Pd 7.87%; **A5**, $RhPd_{0.5}$: Rh 6.96%, Pd 3.28%; **A6**, $RhPd_{0.2}$: Rh 6.30%, Pd 1.20%; **A7**: Rh 5.00%; **A8**, $RhPd_{5.8}$: Rh 1.23%, Pd 7.69%.

TEM samples were prepared by the slow evaporation in a glove box of one drop of a diluted solution of the product in methanol, deposited on a carbon coated copper grid. Reproducible HREM images were obtained from samples produced by independent syntheses. The experiments on $RhPd_{1.5}$ were performed on a Philips CM 30/ST operated at 300 kV with a point resolution of 0.19 nm. HRTEM images of isolated particles were digitized at a resolution of 0.03 nm $pixel^{-1}$ and analysed using their numerical diffractograms (Fourier transforms). TEM of the particles in MeOH solution under H_2 and after catalysis was performed on a JEM 2010 operating at an accelerating voltage of 200 kV with a point resolution of 0.23 nm. Samples were prepared in a glove box under argon and were examined at a magnification between 100 and 400 K. For each sample, and due to the small size of the particles, the diameters of a large number of particles were determined from enlarged photoimages in order to obtain a statistically good size distribution (nearly 200 particles).

Solid samples for WAXS experiments were introduced into thin-walled Lindemann capillaries of 1.5 mm diameter in a glove box filled with argon; the capillaries were sealed for the experiments. Measurements were carried out as previously described.[6,7] Reproducible WAXS patterns were obtained from samples produced by independent syntheses.

IR spectroscopy of adsorbed CO

The colloid (15 mg) was dissolved in CH_2Cl_2 under argon so that the total content of metallic atoms was 6 mmol L^{-1}. The solution was treated with CO (5 bar), stirred for 30 min at room temperature to stabilize the system and then vented. IR spectra were recorded by a Perkin-Elmer Spectrum GX using a CaF_2 cell (1 mm).

Catalysis experiments

Hydrogen C-grade was supplied by Air Liquide. The catalytic reactions were carried out in a 250 mL Fisher–Porter bottle connected to a H_2 tank, and maintained at 40 °C in an oil bath. GC analyses were performed on a HP 4890, equipped with a 25QC5/BPX5 (25 m) column for the hydrogenation of quinoline, and with a Nukol phase column (Supelco 15 m) for the hydrogenation of phenylacetylene. The small size of the particles exclude the presence of internal mass transfer limitations. The first-order reaction, in respect to the solid catalyst, confirms the absence of external mass transfer limitations. The [catalyst]/[substrate] ratio (1/270 or 1/1000) was calculated according to the global concentration of Pd and Rh atoms contained in the [Rh-Pd/PVP] catalyst. In a typical experiment, colloids (11.1 mg of **A5**) and de-ionized H_2O (5 mL) were stirred at 1000 rpm for 20 min until complete dissolution of the catalyst took place. Then, 10 mL of a solution of quinoline (0.3 mol L^{-1}) in CH_2Cl_2, containing tetradecane as internal standard, are added and H_2 admitted (7 bar). Samples of the organic phase were removed from time-to-time for GC analysis. The catalyst was easily separated by decanting the aqueous phase.

Acknowledgements

We thank E. Snoeck (CEMES) for providing HREM facilities and V. Colliere for technical assistance. We are grateful to the CNRS for financial support.

References

1 (*a*) J. Schulz, A. Roucoux and H. Patin, *Chem. Commun.*, 1999, 535; (*b*) J. Schulz, A. Roucoux and H. Patin, *Chem. Rev.*, 2002, **102**, 3257; (*c*) J. Schulz, S. Levigne, A. Roucoux and H. Patin, *Adv. Synth. Catal.*, 2002, **344**, 266; (*d*) H. Bönnemann, W. Brijoux, K. Siepen, J. Hormes, R. Franke, J. Pollmann and J. Rothe, *Appl. Organomet. Chem.*, 1997, **11**, 783; (*e*) T. Yonezawa, in *Morphology Control of Materials and Nanoparticles, Advanced Materials Processing and Characterization Of Well Dispersed Bimetallic Nanoparticles*, ed. Y. Waseda and A. Muramatsu, Springer-Verlag, 2004, pp. 85; (*f*) H. Bönnemann, G. Braun, W. Brijoux, K. Brinkmann, A. S. Tilling, K. Seevogel and K. Siepen, *J. Organomet. Chem.*, 1996, **520**, 143; (*g*) H. Bönnemann and R. M. Richards, *Eur. J. Inorg. Chem.*, 2001, 2455; (*h*) Z. Yu, S. Liao, Y. Xu, B. Yang and D. Yu, *J. Mol. Catal.*, 1997, **120**, 247; (*i*) R. Brayner, G. Viau and F. Bozon-Verduraz, *J. Mol. Catal.*, 2002, **182**, 227; (*j*) K. Philippot and B. Chaudret, *C. R. Chim.*, 2003, **6**, 1019; (*k*) F. Humblot, M. A. Cordonnier, C. Santini, B. Didillon, J. P. Candy and J. M. Basset, in *Studies in Surface Sciences and Catalysis Heterogeneous Catalysis and Fine Chemicals IV*, Elsevier, Amsterdam, 1997, pp. 108; (*l*) *Clusters and Colloids, From Theory to Applications*, ed. G. Schmid, VCH, Weinheim, Germany, 1994; (*m*) *The Chemistry of Nanomaterials: Synthesis, Properties and Applications*, ed. C. N. R. Rao and A. Müller, Wiley-VCH, Weinheim, Germany, 2004; (*n*) *Les Nanosciences 2. Nanomatériaux et Nanochimie*, eds. M. Lahmani, C. Bréchignac and P. Houdy, Collection Echelles, Belin, Paris, 2006.

2 (*a*) B. Bin and N. Toshima, *Chem. Express*, 1990, **5**, 721; (*b*) M. Harada, K. Asakura, Y. Ueki and N. Toshima, *J. Phys. Chem.*, 1993, **97**, 10742.

3 (*a*) *Comprehensive Organometallic Chemistry II: Vol. 12. Transition Metal Organometallic in Organic Synthesis*, ed. E. W. Abel, F. G. A. Stone, G. Wilkinson and L. S. Hegedus, Pergamon Press, Oxford, 1995; (*b*) *Comprehensive Coordination Chemistry II: Vol. 9. Applications of Coordination Chemistry*, ed. J. A. McCleverty, T. J. Meyer and M. D. Ward, Elsevier-Pergamon, Oxford, 2004.

4 (*a*) R. Choukroun, D. de Caro, S. Matéo, C. Amiens, B. Chaudret, E. Snoeck and M. Respaud, *New J. Chem.*, 1998, **22**, 1295; (*b*) R. Choukroun, D. de Caro, B. Chaudret, P. Lecante and E. Snoeck, *New J. Chem.*, 2001, **25**, 525; (*c*) J. L. Pellegatta, C. Blandy, V. Colliére, R. Choukroun, C. Lorber, B. Chaudret, P. Lecante and E. Snoeck, *New J. Chem.*, 2003, **27**, 1528; (*d*) W. Wójtkow, A. M. Trzeciak, R. Choukroun and J. L. Pellegatta, *J. Mol. Catal.*, 2004, **224**, 81.

5 Under the same HREM experimental conditions, diffractograms of Rh and Pd colloids of nearly the same size were previously obtained.

6 M. Bardaji, O. Vidoni, A. Rodriguez, C. Amiens, B. Chaudret, M.-J. Casanove and P. Lecante, *New J. Chem.*, 1997, **21**, 1243.

7 (*a*) A. Rodriguez, C. Amiens, B. Chaudret, M.-J. Cazanove, P. Lecante and J. S. Bradley, *Chem. Mater.*, 1996, **8**, 1978; (*b*) M.-J. Casanove, P. Lecante, E. Snoeck, A. Mosset and C. Roucau, *J. Phys. III*, 1997, **7**, 505.

8 N. Toshima and T. Yonezawa, *New J. Chem.*, 1998, 1179.

9 Geminal $Rh(CO)_2$ (2064 and 1988 cm^{-1}), terminal RhCO (2000 cm^{-1}) and bridged Rh_2CO (1854 cm^{-1}) bands, the geminal and terminal frequencies corresponding to Rh(I) and Rh(0) species, respectively.[9a] Geminal (2059 and 1981 cm^{-1}) and terminal (2017 cm^{-1}) species for PVP-Rh colloids in ethanol as solvent.[9b] The same frequencies were reported for Pd nanoparticles formed in block copolymer micelles.[9c] (*a*) K. Siepen, H. Bönnemann, W. Brijoux, J. Rothe and J. Hormes, *Appl. Organomet. Chem.*, 2000, **14**, 549; (*b*) A. Borsla, A. M. Wilhelm and H. Delmas, *Catal. Today*, 2001, **66**, 389; (*c*) L. M. Bronstein, D. M. Chernyshov, I. O. Volkov, M. G. Ezernitskaya, P. M. Valetsky, V. G. Matveeva and E. M. Sulman, *J. Catal.*, 2000, **196**, 302.

10 P. E. Cattermole, G. Osborne and J. L. Kruczynski, *Inorg. Synth.*, 1977, **17**, 115.

11 (*a*) J. D. Aiken III and R. G. Finke, *J. Mol. Catal. A: Chem.*, 1999, **145**, 1; (*b*) R. W. J. Scott, A. K. Datye and R. M. Crooks, *J. Am. Chem. Soc.*, 2003, **125**, 3708; (*c*) H. Bönnemann, W. Brijoux, R. Brikmann, R. Frezen, T. Joussen, R. Köppler, P. Neiteler and J. Ritcher, *J. Mol. Catal.*, 1994, **86**, 129; (*d*) H. Bönnemann and R. M. Richards, *Eur. J. Inorg. Chem.*, 2001, 2455; (*e*) R. Raja, G. Sankar, S. Hermans, D. S. Shephard, S. Bromley, J. M. Thomas and B. F. G. Johnson, *Chem. Commun.*, 1999, 1571; (*f*) V. Ponec and G. C. Bond, in *Catalysis by Metals and Alloys; Studies in Surface Science and Catalysis*, vol. **95**, Elsevier, Amsterdam, 1995.

12 J.-L. Pellegatta, C. Blandy, V. Collière, R. Choukroun, B. Chaudret, P. Cheng and K. Philippot, *J. Mol. Catal.*, 2002, **178**, 55.

13 The biphasic system is not effective in this case owing the formation of an emulsion due to high concentration of substrate used in the catalysis: 0.30 mol L^{-1}.

14 The quantity of Rh atoms needed to cover the Pd core with a monolayer of Rh atoms can be calculated from the average particle size (1.9 nm). On the basis of a cuboctahedral model and the apparent size of the particles, a four shell cluster of 309 atoms is predicted. A theoretical number of roughly 150 atoms of Rh are necessary to cover the 150 atoms of the Pd core. For the specific $RhPd_4$ bimetallic nanoparticles, nearly 60 atoms of Rh are present in the theoretical total amount of 309 atoms in the particles. This suggests that Rh atoms are located in the outer core and preferentially in a specifically accessible position to the catalytic process, such as an apex or edge, if we speculated further on this issue.

15 H. Bönnemann, W. Brijoux, R. Brinkmann, R. Fretzen, T. Joussen, R. Köppler, B. Korall, P. Neiteler and J. Ritcher, *J. Mol. Catal.*, 1994, **86**, 129.